20

Experimental and Theoretical Analyses of Synchrony in Feedforward Networks

Alex. D. Reyes

ABSTRACT

A hallmark of neural activity during a seizure is the appearance of synchronous events throughout the brain. Synchrony, however, is not exclusively found during a seizure but seems to be ubiquitous under normal conditions and, indeed, may be crucial for information processing. This chapter focuses on recent experimental and theoretical studies of synchrony in feedforward neural networks. This network is the backbone for information transfer in the brain given that signals must be propagated from neuron to neuron, from one nucleus to another, and from one brain region to another. Epileptiform activity may represent an aberrant manifestation of functional synchrony. If so, then understanding the mechanism by which synchrony propagates normally through a neural network might provide clues as to how the synchrony becomes pathological and may suggest preventive measures. As in feedforward networks, epileptiform activity originates from a focal point and then spreads rapidly in a stereotypic manner through a sequence of cortical areas. The simplicity of the feedforward network means that both experimental and rigorous theoretical approaches can be used to derive very general principles, which may then be applied to the study of epilepsy.

INTRODUCTION

SYNCHRONY IN THE NORMAL BRAIN

There is a wealth of electrophysiological evidence suggesting that synchronous firing of neurons is present in the normal functioning brain. Recordings in awake animals reveal synchronous discharges occur, e.g. when animals are exploring space (Csicsvari et al., 1999), performing olfactory discrimination (Stopfer et al., 1997; Martin et al., 2004), motor (Riehle et al., 1997; Hatsopoulos, 1998), visual (Azouz and Gray, 1999, 2003) and memory-related (Sakurai and Takahashi, 2006; Uhlhaas and Singer, 2006) tasks. Synchrony is also postulated to play an important role in generating stereotypical firing patterns in cortex (Ikegaya et al., 2004). Convincing evidence for the presence of synchrony also comes from recent intracellular recordings *in vivo* (Azouz and Gray, 2003; Ikegaya et al., 2004; Bruno and Sakmann, 2006). These experiments reveal the presence of very large voltage transients whose amplitudes often exceed 10 mV, far greater than the 0.3–1 mV unitary synaptic potentials documented between two connected neurons (Markram et al., 1997; Reyes et al., 1998; Reyes and Sakmann, 1999). Therefore, the large transients are likely to be due to the summation of many unitary events that occur synchronously.

Although synchrony is prevalent, its function is still hotly debated. Synchrony has been postulated to be the substrate for encoding precise timing of action potentials that is necessary for pattern formation (Abeles, 1991) or for 'binding' activities of neurons that encode distinct features of a stimulus (Engel and Singer, 2001; Singer, 2001; but see Shadlen and Movshon, 1999). Intracellular recordings *in vivo* reveal that stimulus driven activity is often associated with the appearance or increase in the frequency of synchronous potentials. Experiments with the iteratively constructed networks (see below) suggest that synchrony is crucial for the propagation of information about input rate (Reyes, 2003). In the absence of synchrony, the firing rate (F) at successive layers (L) can be described by: $F_{L+1} = kF_L$ where k is a constant

whose value depends on several parameters including the number of presynaptic inputs, the size of synaptic currents and the input-output transfer function of each neuron. Thus, F is preserved across layers only if the various parameters are such that $k = 1$; otherwise F will either die out ($k < 1$) or blow up ($k > 1$). In the synchronous mode, where frequency is encoded as the inverse of the time between synchronous events, F is propagated more reliably because the large transient potentials are considerably less sensitive to potential variability across layers.

SYNCHRONY DURING SEIZURES

Electroencephalographic (EEG) recordings in patients reveal stereotypical firing patterns during a seizure (see McCormick and Contreras, 2001 for a review). EEG recordings detect the *net* transmembrane current generated by the synaptic activity of a large population of synchronously firing neurons; waveforms from neurons firing asynchronously cancel out. During a seizure, EEG records are characterized by high frequency discharges (tonic) followed by lower frequency transients (clonic). In between seizures are interictal discharges, which consist of brief (100–200 ms) depolarizations that occur periodically. The waveforms are mediated by network synaptic interactions.

Epileptiform activity resembling that observed *in vivo* can be induced in the *in vitro* brain slice preparation. Seizures are commonly generated in the slice by increasing the overall excitability of the neural network. Methods for this include bathing the slice in high K^+ solutions, blocking $GABA_A$-mediated inhibitory inputs, blocking K^+ channels with 4-aminopyridine (4-AP) and removing Mg^{2+} to unveil the N-methyl-D-aspartate (NMDA) components of glutamatergic synapses. Under these conditions, field potential recordings reveal several phases that correspond approximately to those observed in patients: sustained transients during the seizure (ictal) followed by briefer transients (interictal) (Avoli et al., 1996). Intracellular recordings reveal that neurons exhibit large, sustained depolarizations during the ictal phase, characterized by bursts of action potentials riding upon an underlying depolarization (Miles and Wong, 1983; Lopantsev and Avoli, 1998a; McCormick and Contreras, 2001). As will be shown below, these are ideal conditions for spreading synchronous firing in feedforward networks.

In vitro recordings indicate that several cortical areas are activated in a feedforward manner. In a slice preparation containing hippocampus and entorhinal cortex (Avoli et al., 1996; Nagao et al., 1996), pharmacologically induced epileptiform activity progresses sequentially from entorhinal cortex to CA3 and then to CA1 of the hippocampus. Moreover, within entorhinal cortex, epileptiform activity originates from layer V and then propagates to the upper layers (Avoli et al., 1996; Jones and Lambert, 1990). The corticothalamic loop, which may provide a feedback regenerative process important for sustaining epileptiform discharges (McCormick and Contreras, 2001), can also be thought of as a feedforward circuit consisting of alternating layers of cortical and thalamic neurons.

In summary, there is strong evidence for spread of synchrony in a feedforward manner during a seizure. An important question is therefore why synchrony that is present during normal brain function becomes uncontrolled during a seizure.

SYNCHRONY IN FEEDFORWARD NETWORKS

RECONSTRUCTING NETWORKS *IN VITRO*

It is very difficult to examine signal processing in cortex, which consists of several classes of pyramidal cells and excitatory and inhibitory interneurons. It is not possible at the moment to monitor the activities of all the cells during e.g. sensory stimulation, nor is it possible to stimulate, under well-controlled conditions, specific neural populations in a manner similar to what would occur under natural conditions.

To circumnavigate these problems, an iterative procedure was developed which essentially permits the reconstruction of the firing of thousands of neurons within a network from the activity of a single recorded neuron (Reyes, 2003). The technique is a hybrid of experiments in brain slices and computer simulations and offers advantages of both. As with simulations, it is possible to vary systematically parameters to explore synchrony under a variety of conditions. However, the networks are effectively comprised of real neurons, rather than simplified models with many assumed parameters. Moreover, the technique allows us to input specific patterns and monitor the associated activities of all the neurons in the network.

Most networks, including those with recurrent excitation and/or feedback inhibition, can be reconstructed *in vitro* using the iterative procedure (Reyes, 2005). However, it is more informative at this stage first to consider a simple feedforward network. Once the general principles are understood with theoretical analyses (see below), the complexity of the network can be gradually increased to resemble the circuitry in cortex (see below).

Iterative procedure

To construct neural networks using the iterative procedure, whole-cell (or intracellular) recording is first established in a neuron. The general strategy is to simulate the activities of neurons in the first layer, use these to generate inputs which will then be delivered to the recorded neuron several times (once for each neuron in the layer) to recreate the firings of neurons in the second layer. The firings of the recorded neuron are then used to calculate inputs that are again delivered to the recorded neuron (which now represents a neuron in the third layer). This procedure is iterated until the activities of the entire network are reconstructed. The detailed procedure is as follows.

The network shown in Figure 20.1A consists of m layers, each with w neurons. The network is sparsely connected so that each neuron has a 0.1 probability of being connected to a neuron in the next layer. The recorded neuron is defined

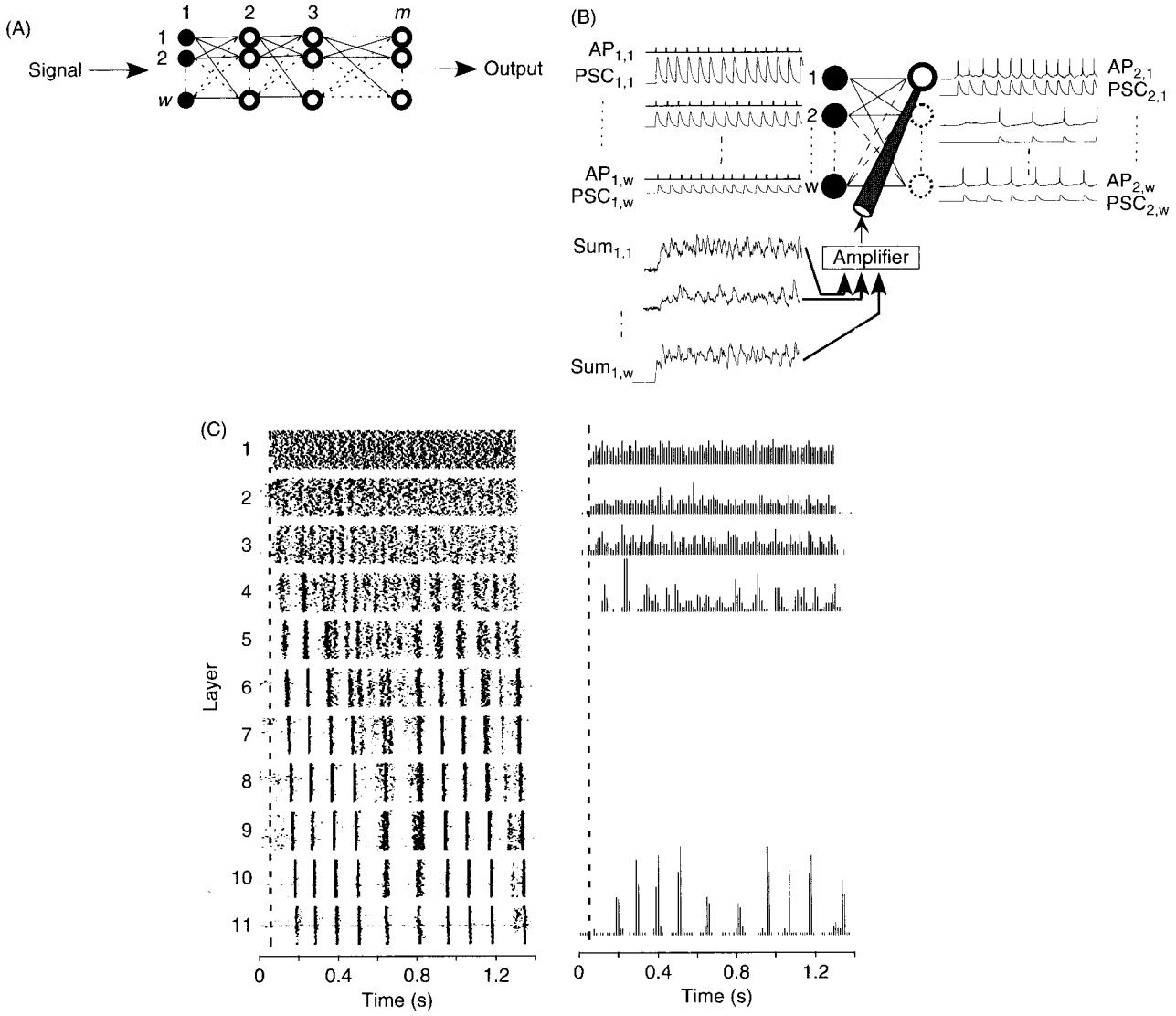

FIGURE 20.1 Synchrony in *in vitro* feedforward networks. (A) Schematic of a feedforward network consisting of m layers with w neurons per layer. (B) Protocol for reconstructing the firing of the neurons in the feedforward network (see text for details). The first layer of neurons is simulated. The spikes are used to calculate synaptic currents (PSCs), which are then injected into the recorded neuron. In the first iteration, the recorded neuron is in the second layer. The neuron is stimulated a total of w times, with each spike train representing the firing of a neuron in the second layer. The amplitudes and latencies of the synaptic currents are randomized. The resultant spike trains are then used to generate synaptic currents, which are re-injected back to the neuron w more times. This reconstructs the firing of neurons in the third layer. This iterative procedure is repeated until the firing of all m layers are re-constructed. (C) Dot rasters of neurons in each layer of an 11-layer network (left). Associated poststimulus time histograms are shown on right. From Reyes (2003).

to be in the second layer (Figure 20.1B). The activities of the w neurons in the first layer are simulated and are made to fire repetitively and asynchronously with respect to each other. Each spike produces a transient that resembles unitary excitatory postsynaptic current (PSC). The amplitude and latency of the PSCs are randomized according to experimentally measured distributions (Markram et al., 1997; Reyes et al., 1998; Reyes and Sakmann, 1999). A subset (10% to reflect the 0.1 connection probability between pyramidal cells) of the trains are chosen at random and summed. The resultant waveform ($sum_{1,1}$, Figure 20.1B) therefore represents the net synaptic current that the layer 1 neurons' combined activity would generate in a layer 2 neuron. This waveform is then injected into the recorded neuron to evoke repetitive firing ($AP_{2,1}$) in one of the cells in the second layer.

Because the network is assumed to be homogeneous, all cells within a layer are identical and differ only in their inputs from the previous layer. Therefore, to replicate the activity of another cell (dashed circles) in layer 2, a new current trace ($sum_{1,2}$) is calculated and injected into the pyramidal neuron once again to evoke repetitive firing ($AP_{2,2}$). The firing is equivalent to another cell in the layer firing. To complete the first iteration, this process is repeated $w-1$ times, once for each neuron in layer 2. To propagate the signal into the third layer, the procedure is repeated except that simulated layer 1 AP trains are replaced with the evoked 'layer 2' AP trains. The summed current is injected into the neuron and the resultant firing is equivalent to that of a cell in the third layer. The pyramidal neuron is once again stimulated $w-1$ times to complete the second iteration. This procedure is iterated $m-1$ times, once for each layer. In this manner, the signal introduced in the first layer could be systematically traced through the network.

DEVELOPMENT OF SYNCHRONY

The most salient feature of activity in the feedforward network is synchrony. In every case examined, synchrony developed by layers 2–3, even though the neurons in the first layer were made to fire asynchronously. Figure 20.1C shows dot rasters, where each row of dots represents a train of APs in a given cell, and the population poststimulus histograms (PSTHs) for each layer of an 11-layer network. In layer 1, the dots in the raster are distributed uniformly and the histogram is flat, reflecting the fact that the simulated neurons fired asynchronously with respect to each other. In layer 2, which is constructed from the activity of real neurons, the dots begin to cluster and the histograms begin to develop peaks indicating that the neurons have started to fire synchronously. With each passing layer, the clustering and histogram peaks become sharper eventually to reach steady-state values.

The development of synchrony is not strongly dependent on the architecture of the network and is indeed robust under a wide variety of configurations. Changing the statistics of the input (from repetitive firing to a Poisson process) or decreasing the connection probability (from 0.1 to 0.01) had little effect on the development of synchrony. To eliminate the possibility that synchrony arose because the network behavior was reconstructed from the activity of only one cell, simultaneous recordings were from up to four cells to make the network more heterogeneous. The neurons were chosen so that their input resistances and firing responses were different: some fired repetitively with different degrees of adaptation, while others fired repetitive bursts. Increasing heterogeneity qualitatively changed the firing patterns but failed to eliminate synchrony. Synchrony also persisted when a random DC bias was introduced from trial to trial to simulate different initial conditions, the PSCs exhibited frequency-dependent changes in amplitudes, and slow NMDA-like PSCs were used.

Synchrony also persisted in the presence of background synaptic noise. The rationale for adding noise to the input is to increase the variability in the timing of action potentials across neurons in a layer. Under *in vivo* conditions, synaptic noise is composed of both excitatory and inhibitory inputs. Inhibitory neurons were incorporated into the iteratively constructed network either by using some of the spike trains of the recorded pyramidal neuron to represent those of inhibitory neurons or to record simultaneously from a pyramidal neuron and an inhibitory interneuron. Excitatory and inhibitory postsynaptic potentials were evoked in the recorded cell by using a dynamic clamp circuit to inject current (Reyes, 2003). Dynamic clamp accurately reproduces the conductance changes caused by synaptic input. Initially, levels of excitatory and inhibitory inputs were adjusted to be in the 'balanced' configuration so that the mixed input increased the variance but not the mean of the injected current. The problem was that firing was difficult to evoke under the balanced configuration because the associated conductances limited the amplitude of the voltage fluctuations; threshold was rarely crossed. Increasing the number of inputs was ineffective because the total conductance of the cell also increased. Similar observations were made during injection of Poisson distributed barrages of excitatory and inhibitory conductances under dynamic clamp (Chance et al., 2002).

Alternatively, the background noise can be injected in current clamp rather than dynamic clamp mode. In current clamp mode, the conductance changes associated with synaptic input are neglected so that the magnitude of the injected current can be arbitrarily large. Injecting noise did reduce synchrony (Reyes, 2003) but only at levels that probably cannot be achieved under physiological conditions (Chance et al., 2002).

Preliminary results with simulations suggest that adding feedback inhibition or recurrent excitation does not remove synchrony (Cateau and Reyes, 2003). In fact, under certain conditions, feedback enhances synchrony. Feedback effectively adds temporal structure to the input due to the fact that there is a fixed latency determined by the axonal length and synaptic delays.

In summary, the experiments show that any network with more than three layers will likely give rise to synchronous firing. It should be noted that inputs were artificially made asynchronous; synchrony will develop faster if the inputs are already partially correlated.

MODELING FEEDFORWARD NETWORKS

The *in vitro* experiments suggest that synchrony is the default state of the feedforward network. In order to devise ways of minimizing synchrony and perhaps, also the rapid spread of epileptiform activity, it is important first to understand the underlying mechanisms that give rise to synchrony. Many of the important principles can be readily understood intuitively with a 'toy' model. A more formal model that uses tools from non-equilibrium statistical physics will be presented below.

TOY MODEL

The development of synchrony in the feedforward networks can in part be explained by two simple phenomena. The first is that with any stimulus, neurons that receive common depolarizing inputs will tend to fire closely in time after the stimulus onset. Stimulus-evoked excitatory inputs into all neurons cause their membrane potential to rise from rest (or any initial conditions) and reach threshold at a rate determined by the membrane time constant. This can be seen readily by modeling the first layer as a network of unconnected leaky integrate-and-fire (LIF) neurons. Numerical simulations of an LIF neuron for a step current give an exponentially rising voltage. Upon reaching threshold, an 'action potential' occurs and the membrane potential is reset back to near rest. Figure 20.2A (left) shows the firing of representative neurons in a layer in response to a current step. Independent noise is added to each neuron to produce variability in spike times. The population PSTH, compiled by summing the individual spike trains, shows a peak shortly after the current step onset followed by progressively smaller peaks. The peak indicates that the spike times tend to cluster at a certain time window; had the spikes occurred randomly with respect to each other, the histograms would be flat.

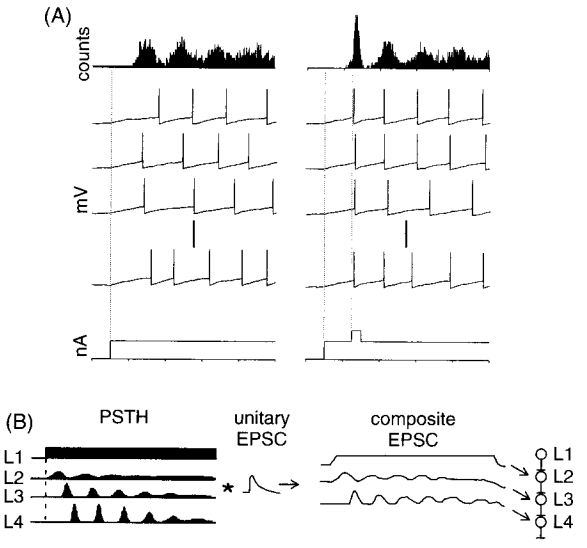

FIGURE 20.2 Mechanisms underlying the development of synchrony. (A, left) Firing simulated with leaky integrate-and-fire neurons. A step of current was injected to each neuron (bottom trace). Noise was added to the voltage to increase spike time variability. The poststimulus time histogram (PSTH) is shown on top. Right, when a brief current transient was added to the step, the peaks in the poststimulus time histogram became taller and narrower. (B) Schematic showing the relation between the PSTH (left) in a given layer and the composite synaptic current that is delivered to the next layer of neurons (right). The composite current is obtained by convolving the PSTH with the unitary postsynaptic current.

The second phenomenon is that any transients in the current will tend to synchronize the cells. As described previously (Perkel et al., 1967; Mainen and Sejnowski, 1995), transient inputs will increase the temporal precision of spikes. This effect can be seen by adding a 'bump' to the step of current (see Figure 20.2A, right). The added pulse causes the membrane potential to rise rapidly to threshold, effectively constricting the distributions of the spikes. The result is that the peaks of the PSTH become narrower and larger. The sharpening of the peaks is magnified if the amplitude and/or rate of rise of the bumps are increased.

These two phenomena provide important clues as to why synchrony increases in successive layers. In the experiments, neurons in the first (simulated) layers were made to fire asynchronously with respect to each other. The resultant PSTH is therefore uniform (see Figure 20.2B). The total input, I(t), to the second layer is essentially the PSTH filtered by the unitary excitatory postsynaptic current (uEPSC). Mathematically, this is equivalent to convolving the PSTH with the uEPSC:

$$I_i(t) = \int PSTH_{i-1}(t) * uEPSC(t-\tau)d\tau \quad (1)$$

Because the PSTH is uniform, the total synaptic current in layer 2 resembles a DC step. As a result, the first phenomenon dictates that the spikes will cluster after a short delay and the PSTH will have peaks. These spikes in turn provide inputs into the third layer. Performing the convolution again shows that the net current into layer 3 neurons will have 'bumps'. Because of the second phenomenon, the resultant PSTHs in layer 3 will have peaks that are narrower and taller. These changes in the PSTHs proceed in successive layers until steady-state synchrony is reached. Note, however, that the toy model, unlike the experiments, predicts that synchrony will decrease with time after the stimulus onset. This discrepancy is examined in greater detail in the next section.

Synchrony propagation was investigated more formally by Diesmann et al. (1999) and by Cateau and Fukai (2001) using idealized state-space analyses. In these modeling studies, the authors delivered a packet of input to the first layer. The packet consisted of spikes that were Gaussian distributed in time. The authors varied the width of the packet (1 standard deviation) and the area (= number of spikes) and examined how the packet propagated through the layers. They ran simulations using different initial values of area and width and then traced the changes in values in a plot of area versus width (idealized state-space graph). There were only two possibilities. If the packet width was sufficiently narrow and the area sufficiently large, the packet propagated successfully. As with the toy model, the packet systematically narrowed to a steady value. In other words, there was an attractor in the state-space graph. On the other hand, if the packet width was broad or the area small so that the initial values were far from the attractor, the packet degraded with successive layers and failed to propagate.

In summary, neurons in a given population will tend to respond within a finite time window after the stimulus onset. This onset synchrony, and the associated peaks that come afterward, provide the seed for synchrony in the next layers. As will be argued below, the onset synchrony is difficult to eliminate under physiological conditions.

FOKKER-PLANCK FORMULATION

To uncover the basic laws that govern the development of synchrony, it is useful to use analyses developed in the physical sciences for analyzing the behavior of large systems of randomly forced particles. Recently, Fokker-Planck equations (FPEs; see Gardiner, 2003) have been applied to the study of feedforward networks (Cateau and Fukai, 2001; Cateau and Reyes, 2005; Doiron et al., 2006). FPEs were originally used by physicists to describe Brownian motion and other diffusive systems. The FPE provides a compact expression that essentially relates the properties of idealized individual neuron models to the behavior of the entire network. Also, from a practical viewpoint, a well-coded FPE program is considerably faster than numerical simulations of large networks of LIF neurons. FPEs may be adapted to neural networks as follows.

For simplicity, each neuron in a layer is modeled as a leaky integrate and fire (LIF) process:

$$\tau_m \frac{dV}{dt} = -V + R_m I_{syn}(t) \quad (2)$$

where V is voltage, τ_m is the membrane time constant and R_m is the membrane resistance. Each i^{th} neuron receives a net synaptic input, $I_{syn}(t)$. As a first approximation, the individual synaptic events that comprise I_{syn} are assumed to be Poisson so that the mean and variance are equal and vary with the input rate. I_{syn} may therefore be described in terms of a diffusion approximation (Gerstein and Mandelbrot, 1964) as:

$$I_{syn}(t) = \alpha N\lambda + \alpha\sqrt{N\lambda}\xi(t) \quad (3)$$

where N is the number of presynaptic cells, α is the total charge produced in the postsynaptic cell by a single presynaptic input (modeled as a δ-function), λ is the input rate, and ζ is the Gaussian white noise term. The first term on the right may be interpreted as the mean synaptic current arriving from neurons in the previous layer and the second term, the fluctuations around the mean.

The evolution of membrane potential of each neuron with time is described by Equation 2. The FPE in turn gives the probability distribution, P(V,t), of membrane potentials of all the neurons in a layer in a slice of time. Figure 20.3A

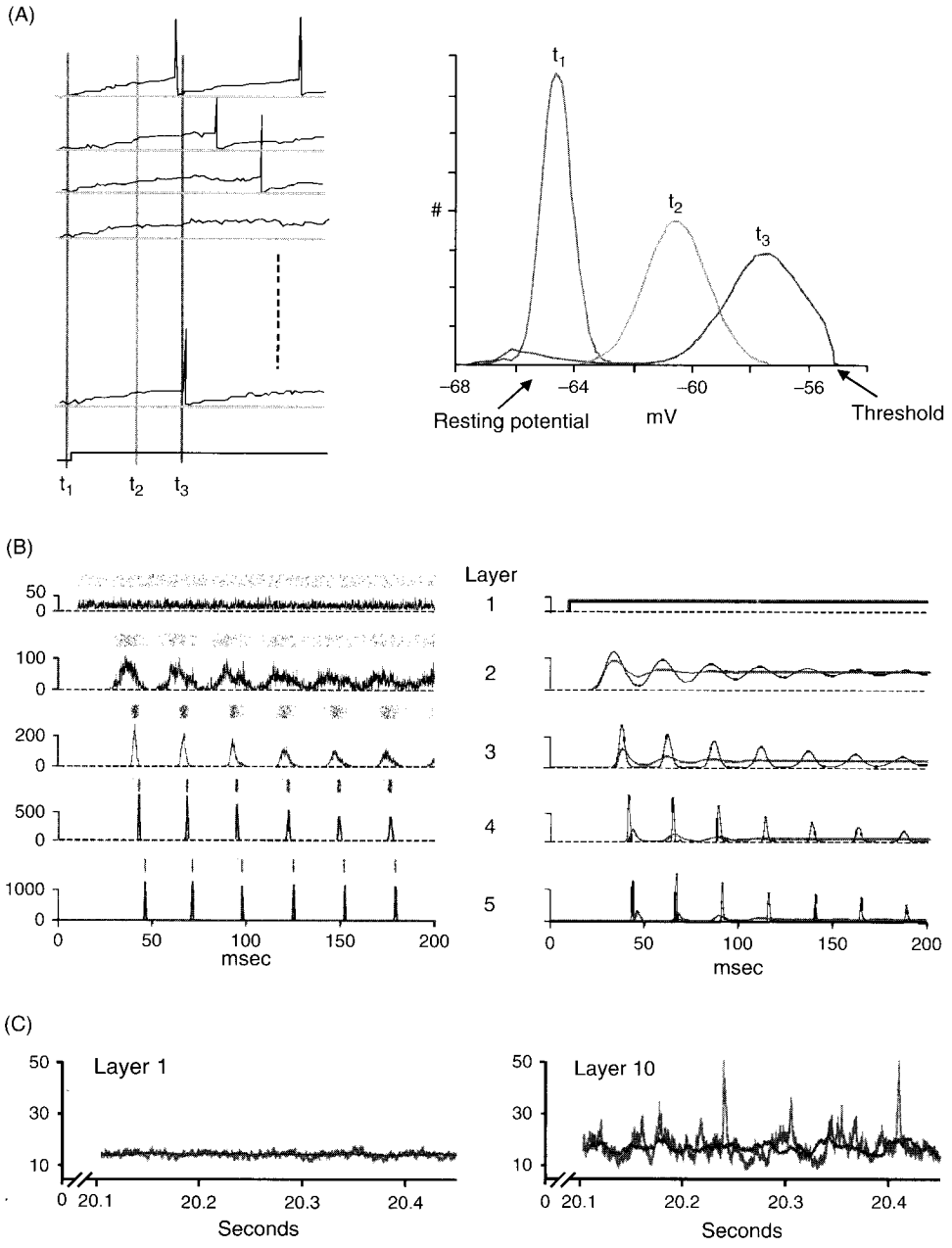

FIGURE 20.3 Fokker-Planck analysis of feedforward networks. (A, left) Firing of a population of leaky integrate-and-fire neurons in response to a current step with Gaussian white noise. Right, distributions of membrane potentials taken through 3 time points (vertical lines on left). (B) Poststimulus time histograms obtained with a feedforward network of leaky integrate and fire neurons. Right, prediction generated with a Fokker-Planck equation assuming that the neurons were Poisson processes (blue). Note that unlike the simulations and experiments, the predicted histogram flattens out by 100 ms, indicating asynchronous firing. Fit to the simulations was improved by relaxing the Poisson assumption (black). From Cateau and Reyes, 2006. (C) Poststimulus time histograms obtained when finite size effect perturbations are taken into account. Synchronous firing persisted when few, larger inputs were used (red). In contrast, asynchrony developed when there were many, small inputs (blue). From Doiron et al., 2006. (See Plate 11 in color plate section.)

(left) shows representative membrane potentials of several LIF neurons in a given layer in response to a step of current. Each neuron receives the same mean current but they do not have identical membrane potentials because of independent sources of noise. Prior to the onset of the stimulus (t_1), the membrane potentials are distributed normally around the resting potential of the neurons (see Figure 20.3A, right, red). Just past the input onset (t_2), the membrane potentials have begun rising and the mean of the distribution shifts rightward toward threshold (green). Note the change in the shape of the distribution. Later in time (t_3), the membrane potentials of a fraction of the neurons have crossed threshold (blue). For simplicity, the action potentials are assumed to be instantaneous and are not registered in the distribution. Hence, the spike reset mechanism forces the distribution to be zero at threshold. After crossing threshold, the membrane potential of the neurons resets and a small peak appears near resting potential. Importantly, the portion of the distribution that crosses threshold gives the firing rate of the population at a given time.

The general FPE is:

$$\frac{\partial P(V,t)}{\partial t} = -a(V,t)\frac{\partial P(V)}{\partial v} + \frac{b^2(V,t)}{2}\frac{\partial^2 P(V)}{\partial V^2} \tag{4}$$

where $P(V, t)$ is the distribution of the membrane potential (V) at a given slice in time (see Figure 20.3A). The term a is the drift term and describes the effects of deterministic forces (i.e. mean synaptic input) on the membrane potential of the population of neurons. The term b is the diffusion term and describes the effects of fluctuating inputs that are statistically identical but statistically independent across the population.

The drift and diffusion terms for the neurons in a given layer can be obtained by combining and re-arranging Equations 2 and 3 to get a stochastic differential equation:

$$\frac{dV}{dt} = \left(-\frac{V}{\tau_m} + \frac{\alpha R_m}{\tau_m}(N\lambda)\right) + \frac{\alpha R_m}{\tau_m}\sqrt{N\lambda}\xi(t) \tag{5}$$

The first term on the right gives the drift term and the second term gives the diffusion term of the FPE:

$$\frac{\partial P(V,t)}{\partial t} = -\left(\frac{V}{\tau_m} - \frac{\alpha R_m}{\tau_m}N\lambda\right)\frac{\partial P(V)}{\partial V} + \frac{N\lambda}{2}\left(\frac{\alpha R_m}{\tau_m}\right)^2\frac{\partial^2 P(V)}{\partial V^2} + J_v(t)\delta(v - V_{reset}) \tag{6}$$

$$\int_{-\infty}^{\infty} P(V,t)dV = 1 \tag{7}$$

where V_{reset} of the flux term corresponds to the depth of the afterhyperpolarization. The flux term has the form:

$$J_V(t) = -\frac{N\lambda}{2}\left(\frac{\alpha R_m}{\tau_m}\right)^2\left.\frac{\partial P(V)}{\partial V}\right|_{v=\theta} \tag{8}$$

The flux term at each time point can be used to construct the PSTH for a given layer. The PSTH, which has units of rate ($= \lambda$), can in turn be used to calculate the drift and diffusion terms for the next layer. The FPE can be solved numerically (Cateau and Reyes, 2005; Doiron et al., 2006) with the boundary condition that $P = 0$ at threshold (reflecting the fact that V is immediately reset to near rest after a threshold crossing).

The FPE as formulated captures some but not all of the important features of synchrony in feedforward networks. Figure 20.3B shows a simulation of a feedforward network of LIF neurons (left) and the PSTHs calculated with the FPE (right, blue) using Equation 6. The FPE-calculated PSTHs, like the simulations, show a gradual development of synchrony in successive layers. However, one major difference is that the peaks of the FPE-calculated PSTH becomes progressively broader with time and eventually flatten out. In contrast, the peaks of the simulated and experimentally determined PSTHs remain robust for the duration of the stimulus.

That the FPE does not fully describe the experimental and simulated data is surprising. *A priori*, the network should behave as a dissipative system and eventually reach equilibrium which, in this case, is asynchrony. The peak at the onset of the stimulus, as argued above, is intuitively clear. However, a reasonable expectation might be that at longer times, the onset synchrony will be 'forgotten' due to cumulative effects of noise. For example, autocorrelation of spike trains *in vivo* or *in vitro* typically exhibit sharp peaks near the origin and progressively broader and flatter peaks later in time (Cateau and Reyes, 2006). This suggests that synchrony in feedforward networks cannot be simply described as a dissipative process; there are other mechanisms that prevent the network from reaching equilibrium.

The discrepancy arises from at least two sources. First, the assumption that the firing of presynaptic neurons, and the associated synaptic currents in their targets, are Poisson processes is incorrect. Neurons are not memory-less but rather tend to fire periodically, as would be expected because neurons have finite membrane time constants and various time-dependent conductances. Indeed, the autocorrelation of spike trains are not δ-functions but rather have troughs on either side of a central peak. It has recently been proven that non-Poisson nature of spiking is preserved even when the activities of an arbitrarily large population of neurons are summed (Cateau and Reyes, 2006; Lindner, 2006). When the Poisson assumption is relaxed, the theory agrees better with the experiments but still shows asynchrony in the large time limit (Cateau and Reyes, 2006). Second, the FPE as formulated in Equation 6 does not take into account for so-called finite size effects. The synaptic potentials are not infinitesimally small so that the histograms in e.g. layer 1 are not smooth but have fluctuations. These fluctuations occur throughout the stimulus and provide 'seeds' for synchrony (in a manner similar to the bumps in the toy model) in the next layer. When the FPE is modified to account for these phenomena, the resultant histograms match the experimental data more accurately and synchrony now persists for all time (Doiron et al., 2006). Figure 20.3C shows that the PSTH obtained with the equivalent of few ($N = 500$) synaptic inputs (red) produced synchrony at long times after the stimulus onset whereas many ($N = 10\,000$) but small synaptic inputs produced a flat PSTH (blue).

In summary, an important implication of the FPE analyses is that once synchrony develops in a particular layer, the network never reaches an equilibrium state where neurons are firing asynchronously. There are 'forcing' functions which are inherent within the network that maintain synchrony for long periods of time.

STRATEGIES FOR ELIMINATING SYNCHRONY

The models suggest that the strategy for reducing synchrony is first to eliminate the tendency of neurons to fire at a fixed delay after the stimulus onset. This tendency causes a peak in the PSTH, which though broad, provides the seed for stronger synchrony in deeper layers. Once a critical number of spikes occurs together in a sufficiently short period of time, full-scale synchrony develops. Secondly, the tendency of neurons to fire at a fixed interspike interval must be reduced. Because neurons tend to fire repetitively, the appearance of the first peak means that there will tend to be another peak approximately one interspike interval (= 1/avg. firing rate) later. Finally, the finite size effects must be reduced. As discussed above, the finite size effects are largely responsible for maintaining synchrony at long times after the stimulus onset.

A completely flat population PSTH occurs when the distribution of spike times for neurons in a layer is uniform. At the onset of the stimulus (for simplicity a step), the membrane potential rises exponentially towards threshold. Thus, the probability that the spike will occur say 3–4 membrane time constants later is much higher than at the start. After spikes occur, the probabilities are again low but will rise back up again (if the stimulus is sustained) and the cycle repeats. Forcing the population spikes to occur randomly is tantamount to making the spiking probability distribution uniform for the entire duration of the stimulus. This is remarkably difficult to accomplish under biological conditions.

One possibility is to make the network functionally more heterogeneous by increasing the distributions of initial conditions of the neurons within a layer. For example, imparting a different subthreshold membrane potential to each neuron would, in principle, cause neurons within a layer to fire spikes at different times with respect to each other (Reyes, 2003). An important restriction is that the distribution of membrane potentials must be uniform across all neurons in a layer. Any peaks in the distribution (as would occur with a Gaussian or Gamma distribution) will cause the population of neurons to fire at a preferred time interval; neurons whose membrane potentials fall e.g. within one standard deviation of the Gaussian will dominate the PSTH. A similar restriction applies to spontaneously active neurons: the distribution of firing frequencies must be uniform.

A second possibility is to increase heterogeneity by e.g. widening the range of membrane properties of the neurons. This was attempted in the experiments but perhaps not enough heterogeneity could be achieved with four types of neurons in the network (see above; Reyes, 2003). The tricky part is choosing a distribution of membrane properties that will produce uniform spiking probabilities. For example, simulations with LIFs indicate that increasing heterogeneity by varying the membrane time constants requires that some neurons have very short time constants (to produce spikes immediately at the start of the stimulus) and some to have very long time constants (to produce spikes at later times). Whether the range of passive (or active) properties of neurons or whether the uniform distribution of these parameters is biologically realistic is unclear.

Eliminating the finite size effects may not be feasible under physiological conditions. This would essentially entail making the amplitude of the synaptic potentials infinitesimally small and the number of presynaptic inputs infinitely large

(Doiron et al., 2006). On the average, the amplitude of EPSPs recorded between pyramidal neurons in rat cortex is about 300 μV to 1 V (Markram et al., 1997; Reyes et al., 1998; Reyes and Sakmann, 1999). Even synaptic inputs located distally in the dendrite could produce a measurable potential at the soma owing to active dendritic conductances that boost the EPSPs (Oviedo and Reyes, 2002, 2005).

The best way of removing synchrony is by introducing background synaptic noise. If the noise is sufficiently large, then the effects of the membrane trajectory both at the stimulus onset and during repetitive firing are reduced substantially. Noise increases the spiking variability of each neuron in the network much more effectively than increasing the heterogeneity or adding feedback, mainly because it causes the neurons to be independent of each other and removes the memory (thereby eliminating peaks following onset synchrony). In the limit, the spikes essentially become Poisson processes. However, the noise amplitude has to be comparable to the difference between resting membrane potential and threshold, which range from 10 to 20 mV. Increasing the variability of the input without changing the mean requires simultaneously increasing the rates of excitatory and inhibitory inputs. As discussed above, producing large amplitude noise may not be possible because the associated increase in synaptic conductance severely limits the amplitude of the fluctuations. *In vivo* recordings do reveal large transients but these, as argued above, are likely to be due to synchronous arrival of inputs. Perhaps a more compelling argument against large amplitude noise is that it would obscure the intended signal, thereby substantially crippling the ability of the network to propagate information.

CONTROLLING THE SPREAD OF SYNCHRONY WITH INHIBITION

Experiments, simulations and theoretical analyses suggest that synchronous firing in feedforward networks is strong and robust under a very wide range of conditions. This raises an obvious question that may have direct implication for epilepsy: what is preventing the synchrony from spreading throughout the cortex? Working under the premise that synchrony is unavoidable and may indeed be necessary for propagating signals, then epilepsy may be viewed as resulting from some malfunction in the ability of the network to control synchrony.

To gain some insights as to how synchrony can spread uncontrollably, the feedforward network must be modified to include realistic connection patterns between neurons in cortex (Marchetti and Reyes, 2004). Holmgren et al. (2003) determined the connection probabilities between pyramidal neurons and between pyramidal and local interneurons in an *in vitro* slice preparation of the rat somatosensory cortex. The study involved painstakingly performing simultaneous whole-cell recording from two neurons and then determining the probability of connection as a function of distance between the cells. An important finding was that pyramidal cells are much more likely to form synaptic connections with interneurons than with each other. On the basis of this study, the connection probability distributions shown in Figure 20.4A were used in the networks. For pyramidal-pyramidal connections, the probability distribution is approximately Gaussian with a peak value of 0.1. In comparison, the pyramidal-interneuron probability distribution is approximately uniform (at least in the limited range examined) with a value of approximately 0.6. Thus, inhibitory neurons, though making up only 20–25% of neurons in cortex, make connections with many of their neighbors within at least 100 μm radius. The connections between pyramidal cells and inhibitory interneurons within and across layers were randomly determined from these distributions. Within each layer, there were recurrent excitatory connections as well as inhibitory feedback. Importantly, the connection scheme effectively set up a lateral inhibitory circuit across layers.

Neurons were modeled using quadratic-integrate-and-fire (QIFs) processes. QIF neurons can be modified so as to produce spiking patterns that resemble those of pyramidal neurons, interneurons or bursting neurons (Izhikevich, 2004). However, for simplicity, the networks were constructed with excitatory and inhibitory neurons that have identical properties. The excitatory and inhibitory synaptic conductances were adjusted to produce EPSPs and IPSPs with amplitudes of approximately 0.5 to 1 mV (see Figure 20.4B, upper traces). Instead of activating the entire first layer as above, stimuli are delivered only to a subset (25%) of the neurons in the center of the first layer.

As with the uniformly connected network above, synchrony developed in the deeper layers. One difference is that the dot rasters tended to be 'C'-shaped. This occurs because neurons at the edge of the stimulus receive less input from the previous layer. Note that neurons at the edge do not fire as synchronously as those in the center.

Preliminary observations suggest that inhibition plays an important role in decreasing the spread of synchrony laterally within each layer (Figure 20.4B, first column). In the control network with both excitatory and inhibitory neurons, the activities in successive layers are confined to a narrow band that matched the extent of the activated neurons in the first layer (dashed lines). When inhibition was removed, the activities in successive layers spread beyond the narrow band (second column).

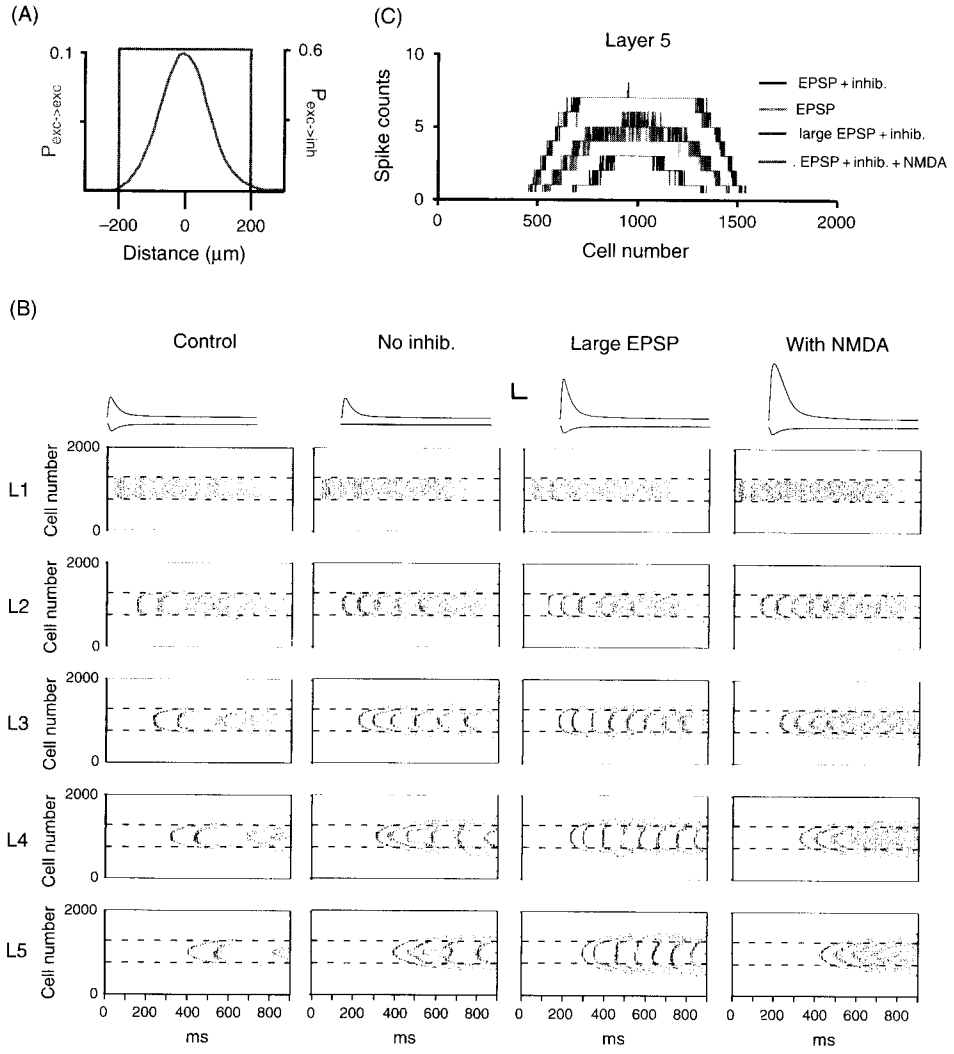

FIGURE 20.4 Spread of synchrony. (A) Probability distributions for connections between pyramidal cells (blue) and between pyramidal cells and inhibitory cells (red) as a function of distance. (B) Dot rasters for 5 layered feedforward networks of quadratic-integrate-and-fire neurons (columns) under 4 configurations (rows). First column: control condition was with excitatory and inhibitory neurons with the connection schemes in (A) (see text). Second column: network with only excitatory neurons. Third column: similar to control network except the amplitude of the excitatory input was doubled. Fourth column: similar to control except an NMDA component was added to the excitatory input. The horizontal dashed lines demarcate the boundary of the activated neurons in layer 1. Scale bars for synaptic potentials: 0.5 mV, 20 ms. (C) Total number of action potentials (ordinate) fired by cells (abscissa) in layer 5 under the 4 conditions. Note that the spread of activity in the non-control conditions was substantially greater than in the control network. (See Plate 12 in color plate section.)

PATHOLOGICAL SYNCHRONY

Synchrony seems to play an important role in signal processing in the normal brain as long as it is confined and controlled. One may imagine many feedforward networks where synchrony exists among neurons within each network but not across networks. Pathology may occur if significant synchrony develops across networks, i.e. when it becomes unbounded. The fact that the tendency to synchronize is so powerful suggests that the nervous system may be teetering on the verge of full-blown synchrony. Small irregularities in the synaptic mechanisms or neural architecture may be all that is needed as a trigger.

Unbounded synchrony may occur when the excitatory/inhibitory ratio increases. A combination of decreased inhibition or increased excitation can attenuate the effectiveness of inhibition at the periphery. As shown above, removing inhibition increases the lateral spread of synchrony. This effect can be enhanced in the control network by doubling the amplitude

of the EPSPs (see Figure 20.4B, third column). Similarly, adding a slow NMDA-like component to the EPSP increases the spread, although the effect appears to be mainly due to the increase in amplitude rather than the longer time course (fourth column). Comparison of the number of action potentials generated by cells in layer 5 shows that increasing the excitatory/inhibitory ratio produces substantially more spread than in the control network (see Figure 20.4C).

Perhaps not surprisingly, the conditions that lead to increased synchrony in feedforward networks are very similar to those that are used in animal models to induce epileptic discharges. Blocking GABA-A receptors with bicuculline and picrotoxin is often used to generate spontaneous depolarizing after hyperpolarization. The protocol for kindling, which involves repetitive stimulation of afferents, is very similar to the protocol for inducing long-term potentiation of excitatory synapses in *in vitro* slice preparations. Unblocking of NMDA receptor mediated potentials by removal of Mg^{2+} would also increase the overall amplitude of EPSPs. The potassium channel blocker 4-AP has the dual effect of increasing the amplitude of EPSPs and depolarizing the cell.

SUMMARY

The default state of feedforward networks is synchronous firing. Even when the input to the first layer is asynchronous, synchrony develops within 2–3 layers. Several factors contribute to synchrony. First, neurons tend to fire at a fixed delay after the stimulus onset, thereby causing a peak in the PSTH. Second, because neurons tend to fire repetitively (i.e. they are non-Poisson processes), multiple peaks form after the onset peak. Third, finite size effects of the networks ensure that synchrony is maintained for all time: theoretical analyses suggest that the neurons within any given layer never reach equilibrium such that there is no asynchronous state. Synchrony is robust and persists for a wide range of network configuration. In the normal brain, it is conceivable that there are many feedforward networks where neurons within but not across networks fire synchronously. Synchrony does not spread owing to the presence of inhibitory neurons. Under pathological conditions, such as when there is a shift in the excitatory/inhibitory ratio, synchrony spreads uncontrollably. Many of the manipulations that promote seizures also facilitate the spread of synchrony in feedforward networks. Much can indeed be learned about the spread of epileptiform activity by studying of simple feedforward networks.

REFERENCES

Abeles, M. (1991). Corticonics. Cambridge University Press, Cambridge.

Avoli, M., Barbarosie, M., Lucke, A., Nagao, T., Lopantsev, V. and Kohling, R. (1996). Synchronous GABA-mediated potentials and epileptiform discharges in the rat limbic system in vitro. J Neurosci 16:3912–3924.

Azouz, R. and Gray, C.M. (1999). Cellular mechanisms contributing to response variability of cortical neurons in vivo. J Neurosci 19:2209–2223.

Azouz, R. and Gray, C.M. (2003). Adaptive coincidence detection and dynamic gain control in visual cortical neurons in vivo. Neuron 37:513–523.

Bruno, R.M. and Sakmann, B. (2006). Cortex is driven by weak but synchronously active thalamocortical synapses. Science 312:1622–1627.

Cateau, H. and Fukai, T. (2001). Fokker-Planck approach to the pulse packet propagation in synfire chain. Neural Netw 14:675–685.

Cateau, H. and Reyes, A.D. (2003). Modulation of synchrony duration in multilayer neural networks by feedback: stochastic analyses. Soc. Neurosci. Abst. 805.2

Cateau, H. and Reyes, A.D. (2006). Relation between single neuron and population spiking statistics and effects on network activity. Phys Rev Lett 96:058101.

Chance, F.S., Abbott, L.F. and Reyes, A.D. (2002). Gain modulation from background synaptic input. Neuron 35:773–782.

Csicsvari, J., Hirase, H., Czurko, A., Mamiya, A. and Buzsaki, G. (1999). Oscillatory coupling of hippocampal pyramidal cells and interneurons in the behaving rat. J Neurosci 19:274–287.

Diesmann, M., Gewaltig, M.O. and Aertsen, A. (1999). Stable propagation of synchronous spiking in cortical neural networks. Nature 402:529–533.

Doiron, B., Rinzel, J. and Reyes, A.D. (2006). Stochastic synchronization in finite size spiking networks. Phys Rev E (rapid comm.) 74.

Engel, A.K. and Singer, W. (2001). Temporal binding and the neural correlates of sensory awareness. Trends Cogn Sci 5:16–25.

Gardiner, C. (2003). Handbook of stochastic methods, 3rd edn. Springer, Berlin.

Gerstein, G.L. and Mandelbrot, B. (1964). Random walk models for the spike activity of a single neuron. Biophys J 4:41–68.

Harris, K.D., Hirase, H., Leinekugel, X., Henze, D.A. and Buzsaki, G. (2001). Temporal interaction between single spikes and complex spike bursts in hippocampal pyramidal cells. Neuron 32:141–149.

Hatsopoulos, N., Ojakangas, C.L., Paninski, L. and Donoghue, J.P. (1998). Information about movement direction obtained from synchronous activity of motor cortical neurons. Proc Natl Acad Sci 95:15706–15711.

Holmgren, C., Harkany, T., Svennenfors, B. and Zilberter, Y. (2003). Pyramidal cell communication within local networks in layer 2/3 of rat neocortex. J Physiol 551:139–153.

Ikegaya, Y., Aaron, G., Cossart, R. et al. (2004). Synfire chains and cortical songs: temporal modules of cortical activity. Science 304:559–564.

Izhikevich, E.M. (2004). Which model to use for cortical spiking neurons? IEEE Trans Neural Netw 15:1063–1070.

Jones, R.S. and Lambert, J.D. (1990). Synchronous discharges in the rat entorhinal cortex in vitro: site of initiation and the role of excitatory amino acid receptors. Neuroscience 34:657–670.

Lindner, B. (2006). Superposition of many independent spike trains is generally not a Poisson process. Phys Rev E Stat Nonlin Soft Matter Phys 73:022901.

Lopantsev, V. and Avoli, M. (1998a). Laminar organization of epileptiform discharges in the rat entorhinal cortex in vitro. J Physiol 509 (Pt 3):785–796.

Lopantsev, V. and Avoli, M. (1998b). Participation of GABAA-mediated inhibition in ictallike discharges in the rat entorhinal cortex. J Neurophysiol 79:352–360.

Mainen, Z.F. and Sejnowski, T.J. (1995). Reliability of spike timing in neocortical neurons. Science 268:1503–1506.

Marchetti, C. and Reyes, A.D. (2004). Using lateral inhibition to control signal flow in iteratively constructed networks. Soc Neurosci Abst 509.3.

Markram, H., Lubke, J., Frotscher, M., Roth, A. and Sakmann, B. (1997). Physiology and anatomy of synaptic connections between thick tufted pyramidal neurones in the developing rat neocortex. J Physiol 500 (Pt 2):409–440.

Martin, C., Gervais, R., Hugues, E., Messaoudi, B. and Ravel, N. (2004). Learning modulation of odor-induced oscillatory responses in the rat olfactory bulb: a correlate of odor recognition? J Neurosci 24:389–397.

McCormick, D.A. and Contreras, D. (2001). On the cellular and network bases of epileptic seizures. Annu Rev Physiol 63:815–846.

Miles, R. and Wong, R.K. (1983). Single neurones can initiate synchronized population discharge in the hippocampus. Nature 306:371–373.

Nagao, T., Alonso, A. and Avoli, M. (1996). Epileptiform activity induced by pilocarpine in the rat hippocampal-entorhinal slice preparation. Neuroscience 72:399–408.

Oviedo, H. and Reyes, A.D. (2005). Variation of input-output properties along the somatodendritic axis of pyramidal neurons. J Neurosci 25:4985–4995.

Oviedo, H. and Reyes, A.D. (2002). Boosting of neuronal firing evoked with asynchronous and synchronous inputs to the dendrite. Nature Neurosci 5:261–266.

Perkel, D.H., Gerstein, G.L. and Moore, G.P. (1967). Neuronal spike trains and stochastic point processes. II. Simultaneous spike trains. Biophys J 7:419–440.

Reyes, A. and Sakmann, B. (1999). Developmental switch in the short-term modification of unitary EPSPs evoked in layer 2/3 and layer 5 pyramidal neurons of rat neocortex. J Neurosci 19:3827–3835.

Reyes, A., Lujan, R., Rozov, A., Burnashev, N., Somogyi, P. and Sakmann, B. (1998). Target-cell-specific facilitation and depression in neocortical circuits. Nat Neurosci 1:279–285.

Reyes, A.D. (2003). Synchrony-dependent propagation of firing rate in iteratively constructed networks in vitro. Nat Neurosci 6:593–599.

Reyes, A.D. (2005). In vitro reconstruction of auditory receptive fields: role of feedforward/back inputs. Soc Neurosci Abst 615.9

Riehle, A.G.S., Diesmann, M. and Aertsen, A. (1997). Spike synchronization and rate modulation differentially involved in motor cortical function. Science 278:1950–1953.

Sakurai, Y. and Takahashi, S. (2006). Dynamic synchrony of firing in the monkey prefrontal cortex during working-memory tasks. J Neurosci 26:10141–10153.

Shadlen, M.N. and Movshon, J.A. (1999). Synchrony unbound: a critical evaluation of the temporal binding hypothesis. Neuron 24:67–77, 111–125.

Singer, W. (2001). Consciousness and the binding problem. Ann NY Acad Sci 929:123–146.

Stopfer, M., Bhagavan, S., Smith, B.H. and Laurent, G. (1997). Impaired odour discrimination on desynchronization of odour-encoding neural assemblies. Nature 390:70–74.

Uhlhaas, P.J. and Singer, W. (2006). Neural synchrony in brain disorders: relevance for cognitive dysfunctions and pathophysiology. Neuron 52:155–168.